

Identification of impact forces on composite structures using an inverse approach

Ning Hu[†]

*Department of Engineering Mechanics, Chongqing University, Chongqing 400044, P.R. China
Department of Aerospace Engineering, Tohoku University, Aramaki-Aza-Aoba 6-6-01,
Aoba-ku, Sendai 980-8579, Japan*

Satoshi Matsumoto[‡], Ryu Nishi^{††} and Hisao Fukunaga^{‡‡}

*Department of Aerospace Engineering, Tohoku University, Aramaki-Aza-Aoba 6-6-01,
Aoba-ku, Sendai 980-8579, Japan*

(Received April 10, 2006, Accepted April 26, 2007)

Abstract. In this paper, an identification method of impact force is proposed for composite structures. In this method, the relation between force histories and strain responses is first formulated. The transfer matrix, which relates the strain responses of sensors and impact force information, is constructed from the finite element method (FEM). Based on this relation, an optimization model to minimize the difference between the measured strain responses and numerically evaluated strain responses is built up to obtain the impact force history. The identification of force history is performed by a modified least-squares method that imposes the penalty on the first-order derivative of the force history. Moreover, from the relation of strain responses and force history, an error vector indicating the force location is defined and used for the force location identification. The above theory has also been extended into the cases when using acceleration information instead of strain information. The validity of the present method has been verified through two experimental examples. The obtained results demonstrate that the present approach works very well, even when the internal damages in composites happen due to impact events. Moreover, this method can be used for the real-time health monitoring of composite structures.

Keywords: impact force; identification; optimization model; PZT; accelerometer.

1. Introduction

It is well-known that carbon fiber reinforced plastic (CFRP) composites possess high specific strength (strength-to-density ratio) and high specific stiffness, and are widely applied to the fields of aerospace, sports, automobiles, constructions, civil engineering, etc. Specifically, the lightness in weight of CFRP, which contributes the improvement of the ability of structures for saving fuel

[†] Associate Professor, Ph.D., Corresponding author, E-mail: hu@ssl.mech.tohoku.ac.jp

[‡] E-mail: matsumoto@ssl.mech.tohoku.ac.jp

^{††} E-mail: nishi@ssl.mech.tohoku.ac.jp

^{‡‡} Professor, E-mail: fukunaga@ssl.mech.tohoku.ac.jp

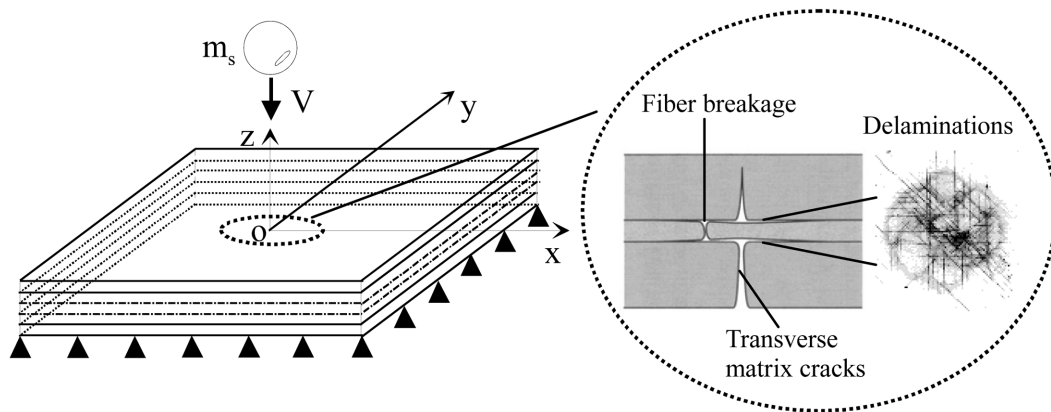


Fig. 1 Various damages due to transverse impacts

consumption, and its very small linear coefficient of thermal expansion make it a kind of widely used materials in structures of aerospace engineering. On the other hand, it is well recognized that this kind of materials is very susceptible to the transverse loads or transverse low-velocity impacts. It has been shown by many researchers, such as Geubelle and Baylor (1998), Duan and Ye (2002), Guinard *et al.* (2002) and Li *et al.* (2002), that low-velocity transverse impact could cause various damages, e.g., as shown in Fig. 1, matrix cracks, delaminations and fiber breakages. Such damages can cause significant reductions in the strength and stiffness of the materials. Especially, the residual compressive strength of laminated CFRP materials with delaminations after the low-velocity impacts (CAI) has been paid much attention in the design of aircraft structures (Wang *et al.* 1995, Hu *et al.* 1999). It has been reported that there are a lot of possibilities to make these damages occur, for instance, the tool drop in the process of production and maintenance of aircrafts, and various collisions between aircraft body and passenger steps, small stones, and flying birds. Such damages are very difficult to be detected by naked eyes in many circumstances. Because under certain loading conditions, these damages may grow rapidly and lead to catastrophic failure of the structures before any precautionary measure can be taken, diagnosis of them is necessary by employing various techniques of damage inspection based on some traditional techniques, such as ultrasonic waves, X-rays, etc. Usually, these kinds of traditional damage inspection techniques cannot be used for the on-line monitoring of structural integrity. Moreover, they are expensive and time-consuming. Accordingly, a new inspection approach, i.e., structural health monitoring, has been recently focused on by many researchers. In this inspection technique, both sensing network and damage inspection algorithm are incorporated into structures and computers, so that structural integrity can be automatically monitored using sensor information. It is known that some important information of external impact forces, e.g., maximum impact force, is tightly related to the damage patterns and damage extents (e.g., Li *et al.* 2002). To establish such a damage-monitoring system for various impact damages, the external impact forces should be first effectively evaluated.

In some previous studies for solving the impact force identification problem, the method using a transfer function that relates the impact forces to the corresponding responses has been proposed. For the cases with given force locations in advance, for example, Inoue *et al.* (1988) have experimentally obtained the transfer function between impact forces and strain responses, and determined the impact forces through the deconvolution method. Using the same relation obtained

numerically, Doyle (1984) proposed a similar technique for identifying an impact force history in a time domain from the strain response of an isotropic beam. This technique was further extended to the identification of impact force in a frequency domain using FFT (Doyle 1987). In addition, the validity of this method was verified through experiments using strain gauges. Wu *et al.* (1994) have constructed Green's functions with the eigenmode expansion method to identify impact force histories by minimizing the residual error between measured strain responses and numerically evaluated ones.

On the other hand, for the impact events without given force locations, some effective methods to identify both locations and histories of impact forces have also been proposed. Yen and Wu (1995) have identified force locations with multiple strain responses on isotropic plates. Impact force histories were identified using the approach by Wu *et al.* (1994). Choi and Chang (1996) have minimized the error between measured strain responses in PZT sensors and numerically evaluated ones to identify impact force locations and histories, simultaneously. Shin (2000) studied the impact force identification technique using the information of modal displacements.

Moreover, some researchers employed the Neural Network to identify impact forces. For instance, Shaw *et al.* (1995) proposed the identification technique of force location and magnitude using the strain measurement of an isotropic plate and Neural Network. Akhavan *et al.* (2000) used the optic fiber and Neural Network to identify the impact forces. For all currently existing methods, it should be noted that so far, no results have been reported for their effectiveness when the practical impact damages happen in structures.

In this paper, a technique to identify the location and history of impact force acting on CFRP laminated plates is proposed. First, the relation between force histories and strain responses in CFRP laminated plates is formulated by using FEM. Next, a reliable identification method of force history and force location is built up. This approach can also be used when acceleration responses are available. Finally, the proposed technique has been realized using an identification system consisting of a measurement part and several signal conditioners. The obtained results show that it is possible to use the present method for the on-line or real-time health monitoring of composite structures, even when impact-induced internal damages in composites occur.

2. Theory

2.1 Strain response induced by impact force

In the low-velocity impact event, a CFRP plate excited by a force in the out-of-plane direction is considered. The governing equation of forced vibration of the plate is described as follows

$$\mathbf{M}\ddot{\mathbf{u}}(t) + \mathbf{C}\dot{\mathbf{u}}(t) + \mathbf{K}\mathbf{u}(t) = \tilde{\mathbf{f}}(t) \quad (1)$$

where \mathbf{M} , \mathbf{C} and \mathbf{K} are the mass matrix, the damping matrix and the stiffness matrix, respectively, $\mathbf{u}(t)$ is the nodal displacement vector, (\cdot) denotes a derivative with respect to time t and $\tilde{\mathbf{f}}(t)$ describes the impact force location and history.

First, in this research, the 4-noded non-conforming bending element based on Kirchhoff plate theory is employed in the FEM model of laminated plates. After performing the natural vibration analysis of Eq. (1), the following mode expansion of displacements can be employed

$$\mathbf{u} = \sum_{i=1}^n \phi_i \xi_i = \Phi \xi \quad (2)$$

where ϕ_i is the i th-order vibration mode, and ξ_i is the i th-order modal displacement.

Then Eq. (1) can be transformed into the modal coordinates as follows

$$\ddot{\xi}_i(t) + 2\zeta_i \omega_i \dot{\xi}_i(t) + \omega_i^2 \xi_i(t) = \phi_i^T \tilde{\mathbf{f}}(t) \quad (3)$$

where ω_i is the i th-order natural circular frequency. And the damping term ζ_i can be expressed as follows

$$\zeta_i = \frac{1}{2} \left(\frac{\alpha_c}{\omega_i} + \beta_c \omega_i \right) \quad (4)$$

when the damping matrix \mathbf{C} in Eq. (1) is cast into the following form

$$\mathbf{C} = \alpha_c \mathbf{M} + \beta_c \mathbf{K} \quad (5)$$

where α_c and β_c are the damping coefficients.

Eq. (3) can be solved by means of Duhamel's integral easily, and then we can obtain the displacement \mathbf{u} by using Eq. (2). Finally, the relation between the impact force history and the strain response measured at the i th sensor can be expressed in the following algebraic equation

$$\tilde{\boldsymbol{\varepsilon}}_i = \mathbf{G}_i \tilde{\mathbf{f}} \quad (6)$$

where the strain and force histories can be expressed at discrete time points as

$$\tilde{\boldsymbol{\varepsilon}}_i = [\varepsilon_i(0) \ \varepsilon_i(\Delta t) \ \dots \ \varepsilon_i(k\Delta t)]^T \quad \text{and} \quad \tilde{\mathbf{f}} = [f(0) \ f(\Delta t) \ \dots \ f(k\Delta t)]^T \quad (7)$$

where $(k+1)$ is the number of sampling points in the time domain.

In Eq. (6), \mathbf{G}_i is a transfer matrix consisting of the Green's function at each time point, which is a lower triangular matrix (Wu *et al.* 1994, Fukunaga and Hu 2004). This matrix is determined by the force location and the observation point of strain only, and is not influenced by the force history.

2.2 Force history identification

The identification of impact force history is discussed in this section. First, an identification technique of force history is built up by solving an inverse problem. When the strain responses are acquired by using the multi-point measurements of sensors, the force history can be obtained by employing the least-squares method in the case of that the force location is known.

When using the FEM to construct the \mathbf{G}_i matrix, however, the direct solution of the identified force history from the traditional least-squares method contains some very large oscillations due to the influence of the FEM modeling errors, measurement noises, etc. Consequently, a technique imposing the penalty on the derivative of the force history is proposed to improve the numerical stability. By applying this technique, the force history can be identified using a minimization problem as

$$\min_{\{\tilde{\mathbf{f}}\}} F = \sum_{i=1}^m \|\boldsymbol{\varepsilon}_i^* - \mathbf{G}_i \tilde{\mathbf{f}}\|^2 + \alpha \|\Delta \tilde{\mathbf{f}}\|^2 \quad (8)$$

subject to $\tilde{\mathbf{f}} \geq \mathbf{0}$

where $\boldsymbol{\varepsilon}_i^*$ is the experimental strain data, m is the number of sensors, α is the regularization parameter for the derivative of the force history, and $\{\Delta \tilde{\mathbf{f}}\} = \mathbf{L} \tilde{\mathbf{f}}$, where \mathbf{L} is a finite difference operator for the first-order derivative of the force history.

It is very important to select a proper regularization parameter α . When the regularization parameter is too small, the identified force history has some very large oscillations. On the contrary, when the regularization parameter is too large, the force history is identified excessively smoothly, and the identified maximum impact force is usually lower than the true one. In this paper, the optimal regularization parameter is determined as a solution of the following maximization problem

$$J = \max_{\alpha} \lambda_{\min}(\mathbf{A}(\alpha)) \quad (9)$$

subject to $\lambda_{\max}(\mathbf{A}(\alpha)) \leq a \lambda_{\max}(\mathbf{A}(0))$

where

$$\mathbf{A} = \sum_{i=1}^m \mathbf{G}_i^T \mathbf{G}_i + \alpha \mathbf{L}^T \mathbf{L} \quad (10)$$

In Eq. (9), $\lambda_{\min}(\mathbf{A}(\alpha))$, $\lambda_{\max}(\mathbf{A}(\alpha))$, and $\lambda_{\max}(\mathbf{A}(0))$ denote, respectively, the minimum and maximum eigenvalues of the matrix \mathbf{A} for an arbitrary α and the maximum eigenvalue of \mathbf{A} for $\alpha=0$. In Eq. (9), the small value of $a=1.01$ is employed here to avoid the excessive change of the maximum eigenvalue of $\mathbf{A}(\alpha)$. A solution of Eq. (9) yields the optimal α . It can prevent the numerical instability due to the maximization of the minimum eigenvalue of $\mathbf{A}(\alpha)$, meanwhile it can avoid excessive smoothing and the extremely lower maximum impact force due to the strict constraint on the change of the maximum eigenvalue of $\mathbf{A}(\alpha)$.

Finally, the force history identification is achieved by solving Eq. (8) by means of the quadratic programming method in this study.

2.3 Force location identification

In this work, another issue is the determination of the force location. In the force history identification with the assumed location, we can obtain a force history denoted by $\tilde{\mathbf{f}}$. Then an error vector, which indicates the deviation between the calculated strains and measured strains, can be defined. The force location is determined by solving the following minimization problem

$$\min_{x,y} E = \sqrt{\sum_1^m \|\boldsymbol{\varepsilon}_i^* - \mathbf{G}_i \tilde{\mathbf{f}}\|^2} \quad (11)$$

Eq. (11) is solved by a nonlinear programming method, e.g., DFP method (Vanderplaats and Sugimoto 1986). In the minimization process, the force history $\tilde{\mathbf{f}}$ is updated using Eq. (8) for each force location. By repeating the above process of solution of Eqs. (8) and (11), we can simultaneously determine the force location and force history.

In the above sections, we have described the relations when using the strain information obtained

from strain sensors. It is also very easy to build up the similar relations using the acceleration information at some points on plates obtained from the accelerometers, and the corresponding theory is abbreviated here for simplicity. In this research, both PZT strain sensors and accelerometers are employed as sensors in our experiments.

3. Identification results

3.1 Verification for CFRP laminates using impulse hammer

To verify the formulations stated in the previous sections, the impact test for CFRP rectangular laminated plates has been performed. The experimental system for verifying the present method is shown in Fig. 2. The identification system consists of a four-corner clamped CFRP plate specimen, a jig, a charge amplifier, a digital oscilloscope, an impulse hammer and a personal computer. Two kinds of CFRP plates are considered in the present research as shown in Table 1. Four specimens were prepared as shown in Table 1 with two kinds of sensors. First, a strain sensor network called SMART Layer (Acellent Technology, Inc.) (Wang and Chang 1999), in which 4 PZT sensors are placed, was utilized to measure strain responses. The schematic illustration of the shape of specimen and sensor positions is in Fig. 3. This SMART layer was embedded within the laminate and near the bottom surface of the plate with the distance of 0.3 mm as shown in Fig. 3. CFRP1 and CFRP3 shown in Table 1 employ this kind of sensors. Also, four accelerometers were used as sensors in this work for CFRP2 and CFRP4 shown in Table 1, which were attached on the top surface of plates. For both kinds of sensors, the sensor locations are shown in Table 2 in the plate plane as shown in Fig. 3. In this test, the impact is applied using an impulse hammer (ONO SOKKI, GK-

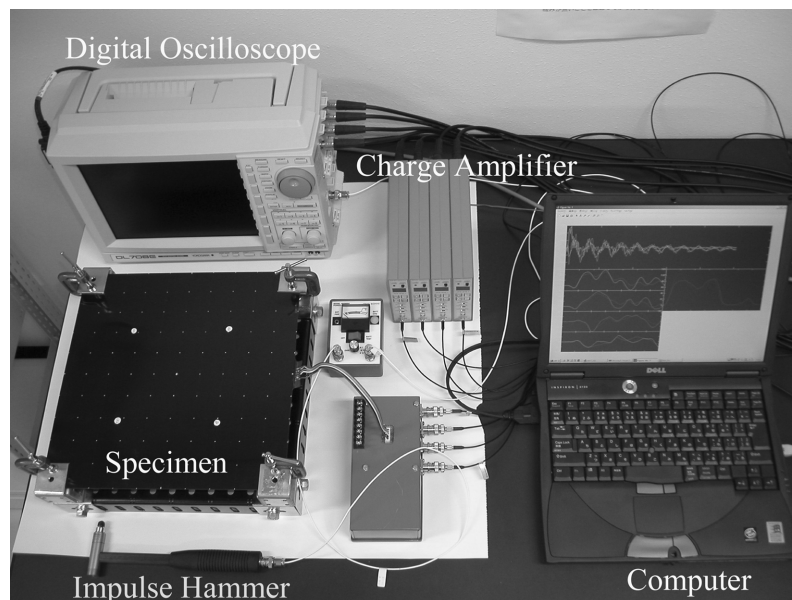


Fig. 2 Experimental system

Table 1 Material properties of specimens

	CFRP1	CFRP2	CFRP3	CFRP4
Sensor	PZT	Accelerometer	PZT	Accelerometer
Laminate sequence	[45 ₂ /-45 ₄ /45 ₂] _s		[0 ₂ /45 ₂ /-45 ₂ /90 ₂] _s	
Geometry [mm]	Length = 300 Width = 300 Thickness = 2.27	Length = 300 Width = 300 Thickness = 2.3	Length = 300 Width = 300 Thickness = 2.3	Length = 300 Width = 300 Thickness = 2.28
E_1 [Gpa]	114.2	104.2	117.6	113.2
E_2 [Gpa]	10.8	10.8	9.2	9.2
G_{12} [Gpa]	5.49	5.49	4.5	4.5
ν_{12}	0.3	0.3	0.3	0.3
ρ [kg/m ³]	1550	1550	1550	1550

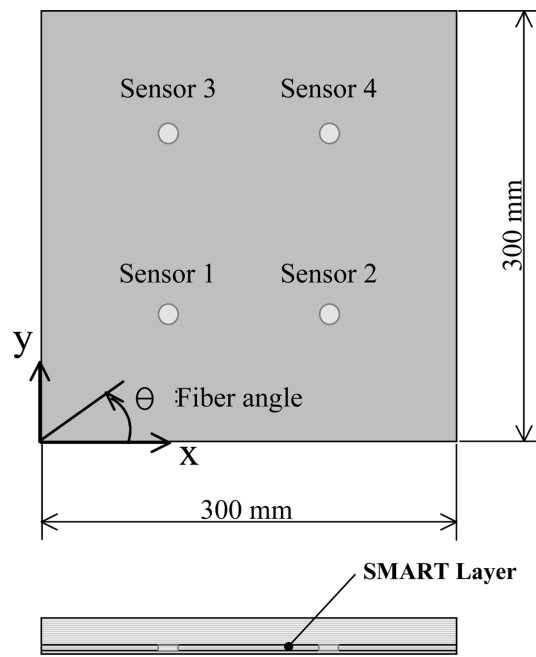


Fig. 3 CFRP specimen and smart layer

Table 2 Sensor positions

Sensor	PZT	Accelerometer
Sensor1	(85 mm, 90 mm)	(90 mm, 90 mm)
Sensor2	(213 mm, 90 mm)	(210 mm, 90 mm)
Sensor3	(86 mm, 216 mm)	(90 mm, 210 mm)
Sensor4	(213 mm, 218 mm)	(210 mm, 210 mm)

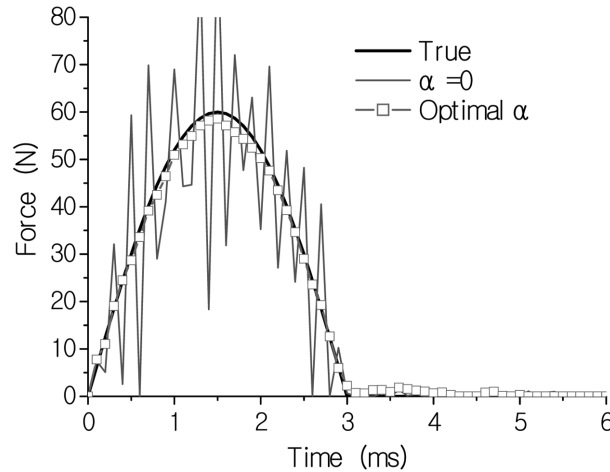


Fig. 4 Relation between regularization parameter and force history

3100). Multiple sensor responses due to the applied impact are amplified through a charge amplifier (ONO SOKKI, CH-1100), and A/D conversion is conducted through a digital oscilloscope (YOKOGAWA, DL708E). Finally, strain or acceleration responses are inputted into a personal computer. The force history is also directly measured from the output of impulse hammer for comparison to the identified force result. When the impact force is applied and the strain or acceleration responses are induced, a trigger signal is sent to the computer from the oscilloscope. After receiving the trigger signal, the computer imports into the strain or acceleration responses from the oscilloscope, identifies the impact force, and then monitors the possible strain or acceleration responses caused by other impact events again. In this test, the measurement time and the sampling time are 1.0×10^{-2} second and 1.0×10^{-4} second, respectively. In order to determine the sensitivity of the PZT sensors, the calibration was performed by comparing the output voltage of the PZT sensor to the output of the biaxial strain gauge located at the same position on the opposite surface of the plate.

First, by employing the numerical simulations for a cantilever plate (CFRP1), we examined the effect of the regularization parameter α in Eq. (8) on the identification results of the force history. To simulate the experimental data, the numerically obtained strain data are mixed with some random noises of 2% of the highest amplitude of response of each sensor. When the force location is specified, the optimal regularization parameter α is determined using Eq. (9). Fig. 4 shows the identified force histories for the optimal value of α and for the value of $\alpha = 0$, which are compared to the true force history. It is shown that the identified force history has some very large oscillations when the regularization parameter is equal to zero. For the optimal regularization parameter, the identified force history agrees very well with the true one.

When using the practical experimental data, Figs. 5(a) and 5(b) show the identification results of the force location for CFRP1 and CFRP3, respectively. The average errors of the identified force locations are 10.2 mm for CFRP1 and 8.5 mm for CFRP3, respectively. The location error is large near the clamped corners or near the free edge of the plate while the error is small in the area existing apart from the boundaries of the plate. The main reason of the location error may be due to the error of FEM modeling. Figs. 6(a) and 6(b) show the identified force histories at the point A for

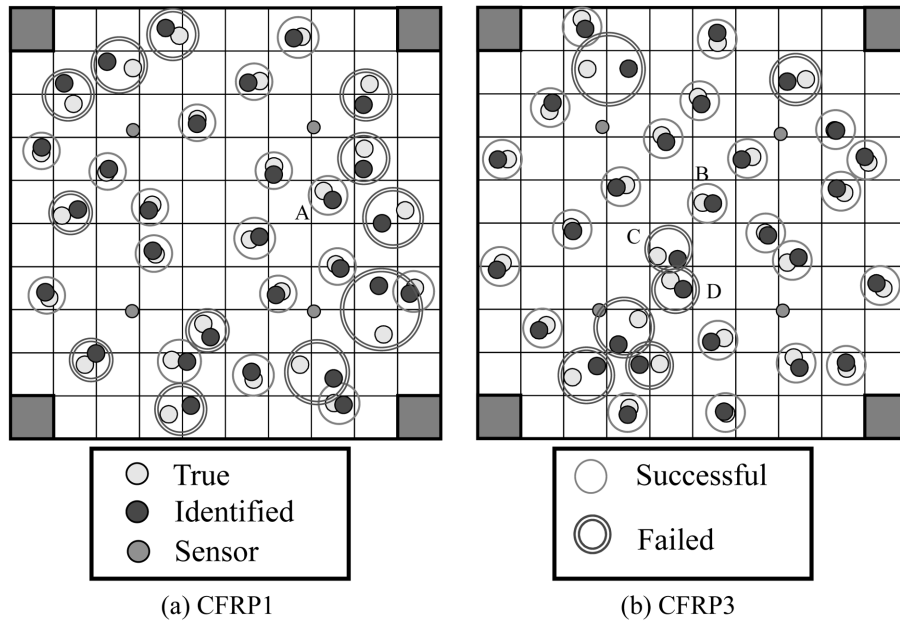


Fig. 5 Identification results of force location using piezoelectrics

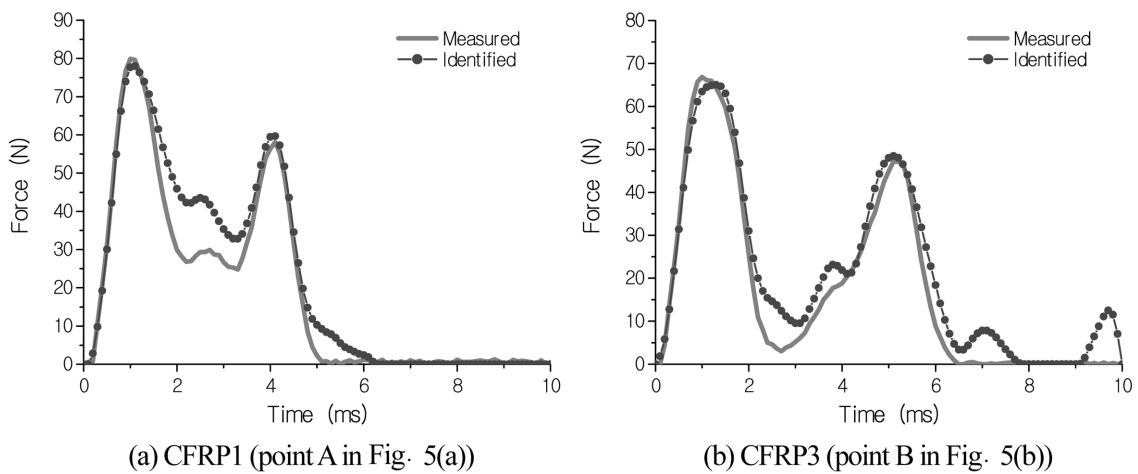


Fig. 6 Results of impact forces using piezoelectrics

CFRP1 and the point B for CFRP3 in Figs. 5(a) and 5(b), respectively. In these cases, the force locations are identified near the true ones. Therefore, the identified force histories agree very well with the experimental ones. When the identified force location is not so accurate, the accuracy of identified impact force history will usually decrease. However, in some cases, although the identification accuracy of force location is not so high, we can also get very accurate results for impact force history, such as the points C and D in Fig. 5(b). Therefore, it can be concluded that the present identification system is very successful for identification of force history and location except at some specified structure boundaries.

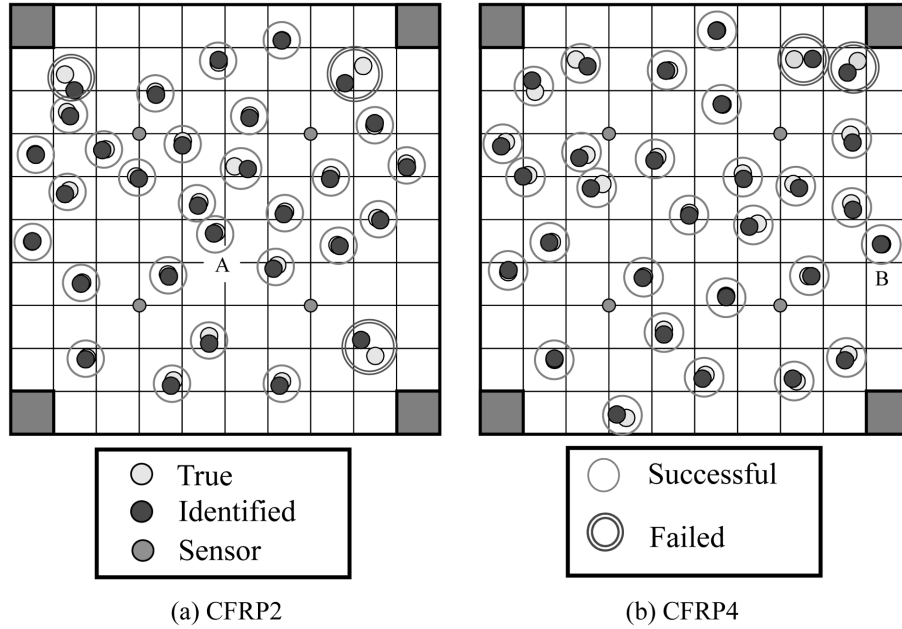


Fig. 7 Identification results of force location using accelerometer

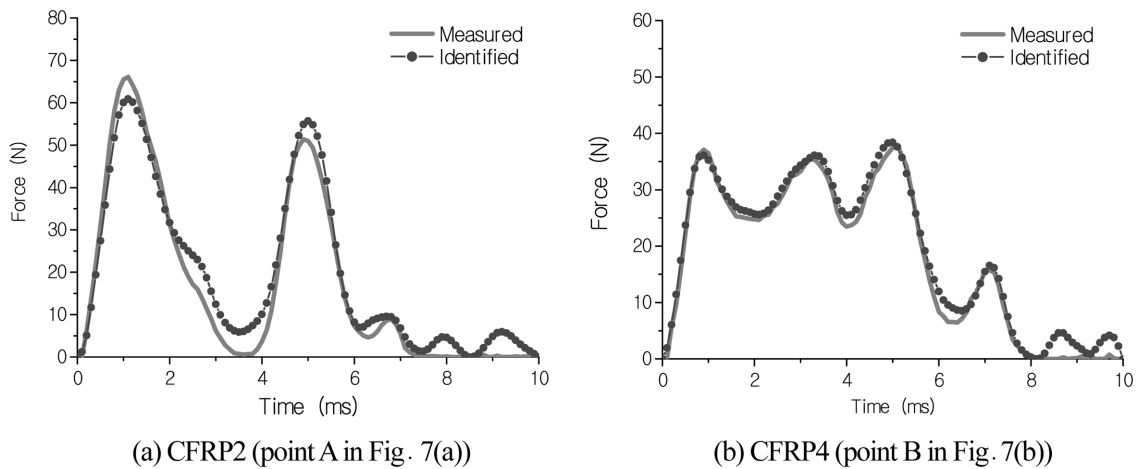


Fig. 8 Results of impact forces using accelerometer

Figs. 7(a) and 7(b) show identification results of the force location for CFRP2 and CFRP4, respectively. The average errors of the force location are 3.8 mm for CFRP2 and 4.2 mm for CFRP4, respectively. Compared to Figs. 5(a) and 5(b), it can be found that the identification accuracy for force location increases remarkably when using accelerometers as sensors. The main reason is that the numerical accuracy of strain data is usually lower than that of acceleration data. Generally, the accuracy of the first-order derivatives of translation displacements for obtaining the strain responses in the FEM model is low. Figs. 8(a) and 8(b) show the identified force histories at the point A for CFRP2 and the point B for CFRP4 in Figs. 7(a) and 7(b), respectively. In these

cases, the impact forces can be identified accurately. Although there is an obvious advantage in the accuracy of accelerometers, the strain sensors are practically employed in more situations due to its small sizes and installation convenience.

For the present method, most of the identification time is required in the search process of force location identification. The force history identification is very fast at a specified force location. To speed up the identification process, in our identification system, the strain responses from four sensors are compared first. When the observable strain signal of a sensor among four sensors arrives first, the force location search is then limited to an area surrounding that sensor (around 1/4 size of the plate). Other portions of the plate will not be searched in our algorithm. In this case, the present force identification system is very fast, which takes only a few seconds to identify the location and the history for each impact event.

3.2 Verification for quasi-isotropic CFRP laminates using drop-weight tests

Another example is a drop-weight test using Dynatup 9250HD test machine made by Instron Inc. The supporting jig and specimen were prepared according to SACMA standards of CAI test as shown in Fig. 9. The rectangular quasi-isotropic CFRP specimen was put on a supporting frame with 4-point fixed on the surface of the specimen. An impactor with the mass of 4.6 kg drops at the center of the specimen. An accelerometer was installed on the impactor to measure the impact force. The dimensions of the quasi-isotropic CFRP of 32 plies $[(45^\circ/0^\circ/-45^\circ/90^\circ)_4]_S$ are shown in Fig. 10 with the material properties defined in Table 3. 4 impact energy levels were investigated as

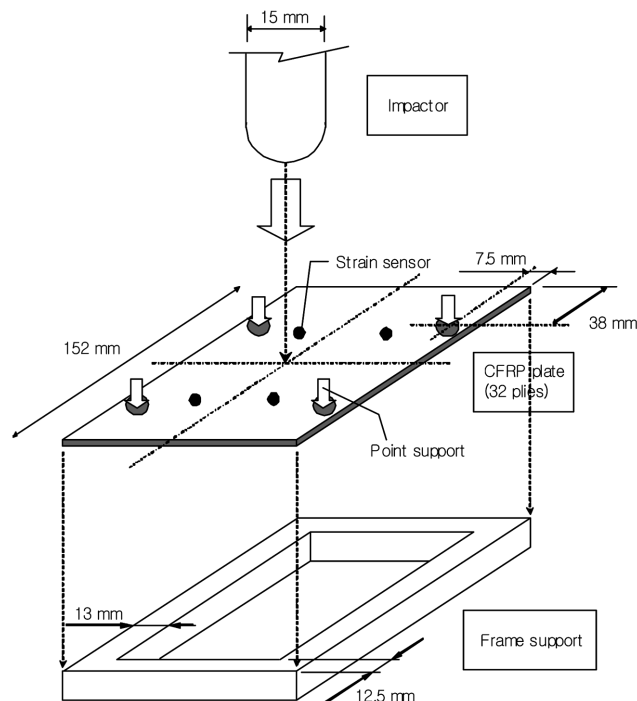


Fig. 9 Drop-weight test setup

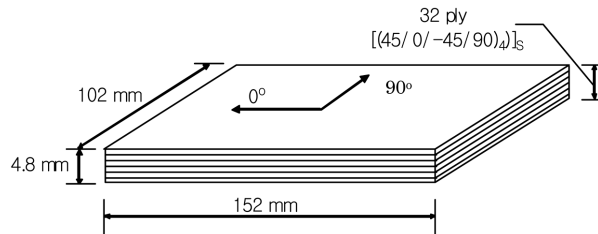


Fig. 10 Quasi-isotropic CFRP specimen

Table 3 Material properties of CFRP specimen

Elastic constants of lamina	
$E_1 = 135.0 \text{ GPa}, E_2 = E_3 = 10.0 \text{ GPa},$ $G_{12} = G_{13} = 5.50 \text{ GPa}, G_{23} = 4.50 \text{ GPa}$ $\nu_{12} = 0.0183, \nu_{13} = 0.45, \nu_{23} = 0.25, \rho = 1489 \text{ kg/m}^3$	

Table 4 Impact test results

Case No.	Impact energy (J)	Damage
1	3.0	none
2	3.0	none
3	4.8	none
4	4.8	damaged
5	6.0	damaged
6	6.0	damaged
7	7.2	damaged
8	7.2	damaged

shown in Table 4. For each energy level, two tests for two specimens were performed. The presence of damages in specimens after impact was checked by ultrasonic inspections. From Table 4, we can find that for the case of 3.0 J, there is completely no damage for two tested specimens. However, for 4.8 J, there are damages in one specimen, meanwhile there is completely no damage in another specimen. When the impact energy is higher than 4.8 J, the impact-induced damages always happen. The force histories in two tests are very similar and repeatable except for the case of 4.8 J. The ultrasonic inspection results of damages of 6.0 J from the top, bottom and thickness direction are shown in Fig. 11. In this example, to construct the \mathbf{G}_i matrix, the FEM model with 384 elements is shown in Fig. 12, in which the four points on the plate surface and the inner edge of the supporting frame are modeled by fixed boundary conditions. Four bi-axial strain gages were attached on the upper surface of plate, with the locations of (31 mm, 46 mm) for Sensor 1, (71 mm, 46 mm) for Sensor 2, (31 mm, 106 mm) for Sensor 3 and (71 mm, 106 mm) for Sensor 4. In the \mathbf{G}_i matrix constructed from the FEM model, no damages are considered. This matrix of the intact plate may cause errors for the cases of high impact energies, such as 6.0 J and 7.2 J, which induce obvious damages. In this research, only impact force history is identified since the impact location is fixed at the center of plate when performing the experiments.

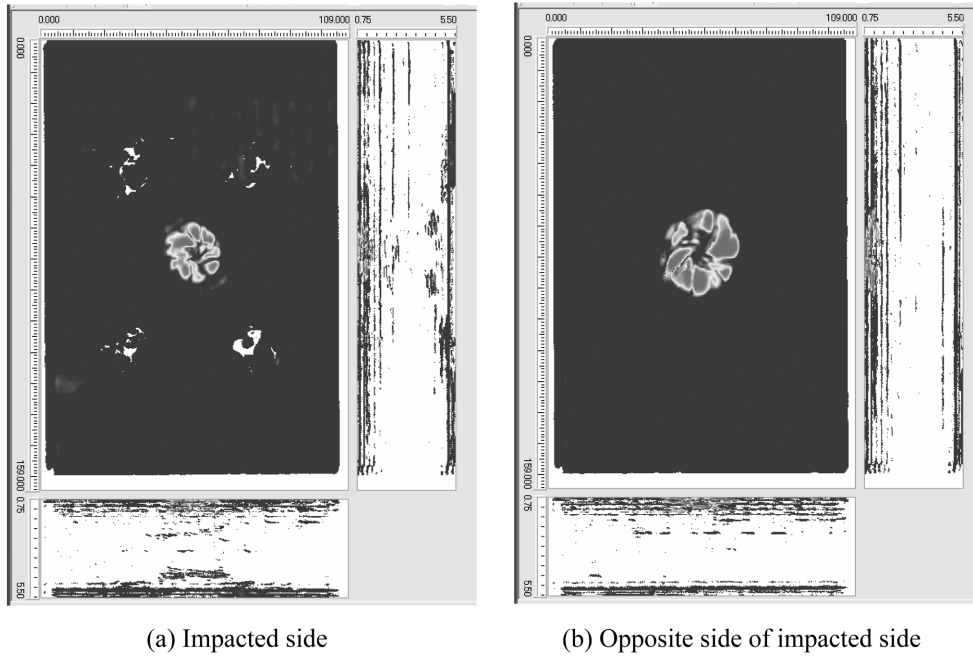


Fig. 11 Results of ultrasonic inspection for 6.0 J

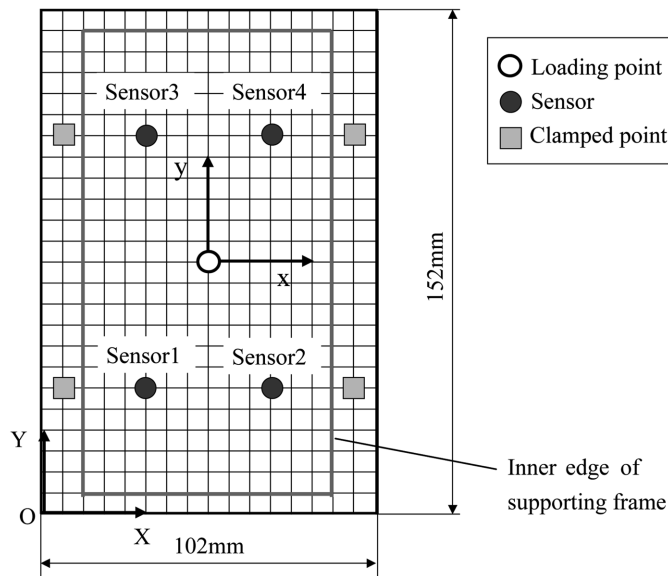


Fig. 12 FEM mesh for identification of impact force

First, for the cases without happening of damages, the results are shown in Fig. 13. From it, we can find that for cases 1 and 2 (3.0 J) and case 3 (4.8 J) in Table 4, the present approach can identify the impact force very accurately. It means that for the cases without damages, the constructed G_i matrix is quite accurate. Second, for the cases with damages, the results are plotted

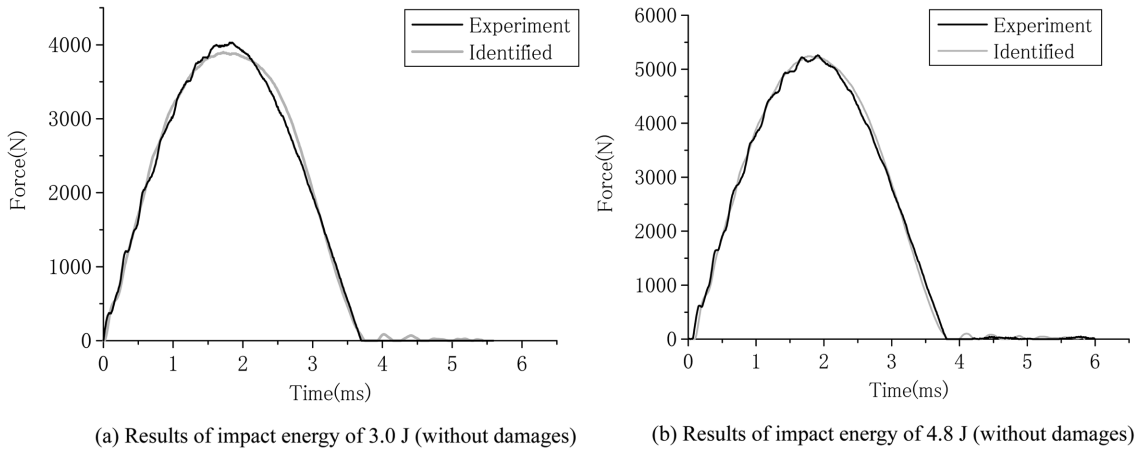


Fig. 13 Identified impact forces for cases without damages

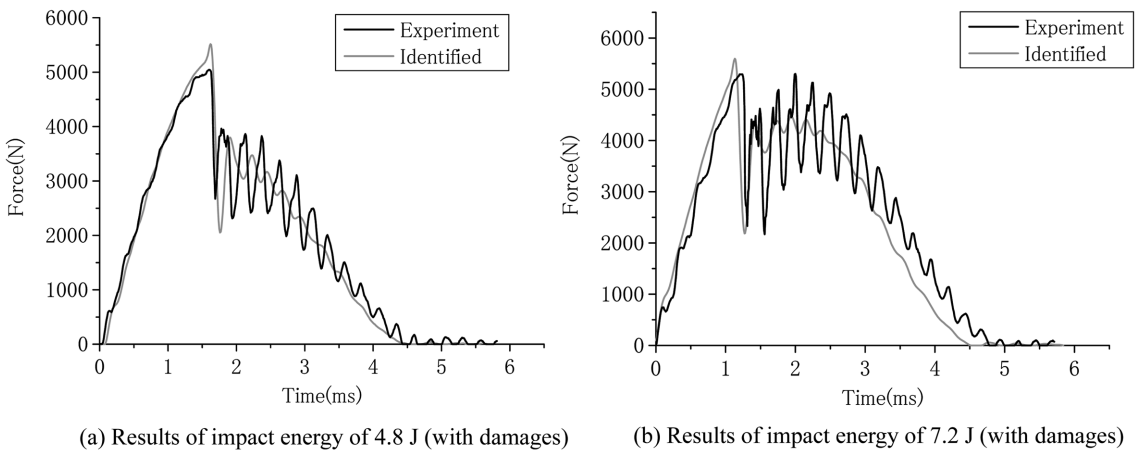


Fig. 14 Identified impact forces for cases with damages

in Fig. 14. In this case, the impact force history becomes more complex. Fig. 14(a) shows that for case 4 (4.8 J) with damages, the present approach can identify the impact force very well. However, at the stage after the peak load, the present approach cannot precisely trace the oscillating curve of experimental one. It seems that after the peak load, the present technique yields the smooth average impact force. In Fig. 14(b), the results for 7.2 J are shown. From it, we can find that the present approach works well. However, compared to Fig. 14(a), the identified result becomes slightly worse due to higher damage extent in this case. The duration of identified impact force is slightly shorter than that of experimental one since the FEM model without consideration of damages may evaluate the higher structural stiffness. This FEM model yields inaccurate \mathbf{G} , matrix at the stage after the occurring of internal impact damages. Although there are some errors in the numerical model for the damaged cases, Fig. 14 illustrates that the present approach is still effective for obtaining acceptable impact force history.

4. Conclusions

In this research, an identification method of impact force acting on composite structures is proposed. First, the transfer matrix, which connects the measured responses of sensors and impact force information, is constructed from the FEM model. Second, the corresponding optimization model to minimize the difference between the measured responses and numerically evaluated responses is built up to obtain the stable impact force history. Moreover, an error vector indicating the force location is defined for searching for the force location. Two experimental examples have been employed to illustrate the validity of the present method. From the results, it can be found that the proposed method can identify the impact force history and location accurately within a few seconds. Therefore, the proposed inverse method can be used for the real-time health monitoring of composite structures. When using accelerometers as sensors, the identification accuracy is higher than that of PZT strain sensors. The errors of identified force location are higher near structure boundaries due to the numerical modeling errors and experimental noises. When the internal damages induced by impact events happen, the accuracy of identified force history is still within the acceptable range. The main problem in the present approach is that the transfer matrix is constructed by the numerical model, which certainly leads to the lower modeling and identification accuracies (e.g., the force location) for complex and large-scale structures. In the ongoing research, this problem will be addressed through constructing a highly reliable transfer matrix experimentally.

Acknowledgements

This work is partly supported by the Award from AFOSR numbered by FA4869-06-1-0076.

References

- Akhavan, F. and Watkins, S.E. *et al.* (2000), "Prediction of impact contact forces of composite plates using fiber optic sensors and neural networks", *Mech. Compos. Mater. Struct.*, **7**, 195-205.
- Choi, K. and Chang, F.K. (1996), "Identification of impact force and location using distributed sensors", *AIAA J.*, **34**, 136-142.
- Doyle, J.F. (1984), "An experimental method for determining the dynamic contact law", *Exp. Mech.*, **24**, 10-16.
- Doyle, J.F. (1987), "Experimentally determining the contact force during the transverse impact of an orthotropic plate", *J. Sound Vib.*, **118**, 441-448.
- Duan, S.H. and Ye, T.Q. (2002), "Three-dimensional frictional dynamic contact analysis for predicting low-velocity impact damage in composite laminates", *Adv. Eng. Softw.*, **33**, 9-15.
- Fukunaga, H. and Hu, N. (2004), "Health monitoring of composite structures based on impact force identification", *Proceeding of the Second European Workshop, Structural Health Monitoring*, Edited by C. Boller and W.J. Straszewski, 415-422.
- Geubelle, P.H. and Baylor, J.S. (1998), "Impact-induced delamination of composites: a 2D simulation", *Composites: Part B*, **29B**, 589-602.
- Guinard, S. and Allix, O. *et al.* (2002), "A 3D damage analysis of low-velocity impacts on laminated composites", *Compos. Sci. Technol.*, **62**, 585-589.
- Hu, N. and Fukunaga, H. *et al.* (1999), "Compressive buckling of laminates with an embedded delamination", *Compos. Sci. Technol.*, **59**, 1247-1260.
- Inoue, H. and Watanabe, R. *et al.* (1988), "Measurement of impact force by the deconvolution method (part-a)", *J. JPN Soc. Non-Destructive Inspection*, **34**, 337-342.
- Inoue, H. and Watanabe, R. *et al.* (1988), "Measurement of impact force applied to a plate by the deconvolution

- method (part-b)", *J. JPN Soc. Non-Destructive Inspection*, **37**, 874-878.
- Li, C.F. and Hu, N. *et al.* (2002), "Low-velocity impact-induced damage of continuous fiber-reinforced composite laminates. Part I. An FEM numerical model", *Composites: Part A*, **33**, 1055-1061.
- Li, C.F. and Hu, N. *et al.* (2002), "Low-velocity impact-induced damage of continuous fiber-reinforced composite laminates. Part II. Verification and numerical investigation", *Composites: Part A*, **33**, 1063-1072.
- Shaw, J.K. and Sirkis, J.S. *et al.* (1995), "Model of transverse plate impact dynamics for design of impact detection methodologies", *AIAA J.*, **33**, 1327-1335.
- Shin, E.S. (2000), "Real-time recovery of impact force based on finite element analysis", *Compos. Struct.*, **76**, 621-627.
- Vanderplaats, G.N. and Sugimoto, H. (1986), "A general purpose optimization program for engineering design", *Comput. Struct.*, **24**, 13-21.
- Wang, C.S. and Chang, F.K. (1999), "Built-in diagnostics for impact damage identification of composite structures", *Structural Health Monitoring 2000, Stanford, 1999*, Edited by F.K. Chang (Stanford University, 1999), 612-621.
- Wang, J.T.S. and Cheng, S.H. *et al.* (1995), "Local buckling of delaminated beams and plates using continuous analysis", *J. Compos. Mater.*, **29**, 1374-1402.
- Wu, E. and Yeh, J.C. *et al.* (1994), "Identification of impact forces at multiple locations on laminated plates", *AIAA J.*, **32**, 2433-2439.
- Yen, C.S. and Wu, E. (1995), "On inverse problem of rectangular plates subjected to elastic impact, Part I: method development and numerical verification", *J. Appl. Mech.*, **62**, 692-698.
- Yen, C.S. and Wu, E. (1995), "On inverse problem of rectangular plates subjected to elastic impact, Part II: experimental verification and further application", *J. Appl. Mech.*, **62**, 699-705.